

# Overview of results in the MST reversed field pinch experiment

S.C. Prager<sup>1</sup>, J. Adney<sup>1</sup>, A. Almagri<sup>1</sup>, J. Anderson<sup>1</sup>, A. Blair<sup>1</sup>,  
D.L. Brower<sup>2</sup>, M. Cengher<sup>1</sup>, B.E. Chapman<sup>1</sup>, S. Choi<sup>1</sup>, D. Craig<sup>1</sup>,  
S. Combs<sup>3</sup>, D.R. Demers<sup>4</sup>, D.J. Den Hartog<sup>1</sup>, B. Deng<sup>2</sup>,  
W.X. Ding<sup>2</sup>, F. Ebrahimi<sup>1</sup>, D. Ennis<sup>1</sup>, G. Fiksel<sup>1</sup>, R. Fitzpatrick<sup>5</sup>,  
C. Foust<sup>3</sup>, C.B. Forest<sup>1</sup>, P. Franz<sup>6</sup>, L. Frassinetti<sup>6</sup>, J. Goetz<sup>1</sup>,  
D. Holly<sup>1</sup>, B. Hudson<sup>1</sup>, M. Kaufman<sup>1</sup>, T. Lovell<sup>1</sup>, L. Marrelli<sup>6</sup>,  
P. Martin<sup>6</sup>, K. McCollam<sup>1</sup>, V.V. Mirnov<sup>1</sup>, P. Nonn<sup>1</sup>, R. O'Connell<sup>1</sup>,  
S. Oliva<sup>1</sup>, P. Piovesan<sup>6</sup>, I. Predebon<sup>6</sup>, J.S. Sarff<sup>1</sup>, G. Spizzo<sup>6</sup>,  
V. Svidzinski<sup>1</sup>, M. Thomas<sup>1</sup>, E. Uchimoto<sup>7</sup>, R. White<sup>8</sup> and  
M. Wyman<sup>1</sup>

<sup>1</sup> Center for Magnetic Self-Organization in Laboratory and Astrophysical Plasmas,  
The University of Wisconsin, Madison, WI, USA

<sup>2</sup> The University of California at Los Angeles, Los Angeles, CA, USA

<sup>3</sup> The Oak Ridge National Laboratory, Oak Ridge, TN, USA

<sup>4</sup> Rensselaer Polytechnic Institute, Troy, NY, USA

<sup>5</sup> The University of Texas, Austin, TX, USA

<sup>6</sup> Consorzio RFX, Associazione EURATOM-ENEA sulla Fusione, Padova, Italy

<sup>7</sup> The University of Montana, Missoula, MT, USA

<sup>8</sup> Princeton Plasma Physics Laboratory, Princeton, NJ, USA

Received 10 December 2004, accepted for publication 15 April 2005

Published 7 October 2005

Online at [stacks.iop.org/NF/45/S276](http://stacks.iop.org/NF/45/S276)

## Abstract

Confinement in the reversed field pinch (RFP) has been shown to increase strongly with current profile control. The MST RFP can operate in two regimes: the standard regime with a naturally occurring current density profile, robust reconnection and dynamo activity; and the improved confinement regime with strong reduction in reconnection, dynamo and transport. New results in standard plasmas include the observation of a strong two-fluid Hall effect in reconnection and dynamo, the determination that the  $m = 0$  edge resonant mode is nonlinearly driven, and the determination that tearing modes can lock to the wall via eddy currents in the shell. New results in improved confinement plasmas include observations that such plasmas are essentially dynamo-free, contain several isolated magnetic islands (as opposed to a stochastic field) and contain reduced high frequency turbulence. Auxiliary current drive and heating is now critical to RFP research. In MST, a programme to apply auxiliary systems to the RFP is underway and progress has accrued in several techniques, including lower hybrid and electron Bernstein wave injection, ac helicity injection current drive, pellet injection and neutral beam injection.

**PACS numbers:** 52.55.Lf

(Some figures in this article are in colour only in the electronic version)

## 1. Introduction

In the MST reversed field pinch (RFP), plasma can be produced in two quite different physics regimes: standard-confinement plasmas with strong reconnection and dynamo activity, and improved confinement plasmas with reduced reconnection, dynamo and transport. In the standard RFP, current-driven tearing instabilities produce magnetic fluctuations that have a large effect on the macroscopic plasma quantities,

causing strong magnetic relaxation phenomena. In the RFP with current density profile control, the plasma is more stable, magnetic fluctuations are reduced, energy confinement increases tenfold and magnetic relaxation phenomena are strongly reduced. Current profile control is enacted transiently in MST through programming of the Ohmic electric field.

In this paper, we report new results on the nonlinear behaviour of fluctuations and their consequences in standard plasmas, and the substantial changes with improved

confinement. In section 2 we report three new results from standard plasmas: observation of the Hall dynamo (and Hall effects on reconnection), measurement of linear damping of the edge resonant  $m = 0$  mode (implying a nonlinear origin for the mode) and measurement that mode braking, in some MST plasmas, is consistent with torques arising from shell eddy currents. In section 3 we report three results in plasmas with improved confinement: the demonstration of dynamo-free plasmas, the observation of isolated magnetic islands (indicating the suppression of magnetic stochasticity) and the reduction of high frequency magnetic turbulence (implying its connection to global tearing modes).

In MST, a set of current drive and heating systems are being developed. The strong increase of plasma confinement with transient current profile control indicates the importance of the development of control tools. In MST, the Ohmic input power, particularly with improved confinement, is sufficiently low that auxiliary power input is now feasible. In section 4 we summarize the progress in RF power input (lower hybrid and electron Bernstein waves), neutral beam injection, oscillating field current drive (OFCD) (a form of ac magnetic helicity injection for bulk current sustainment) and pellet injection.

## 2. Relaxation and fluctuations in standard RFP plasmas

### 2.1. Two-fluid effects on reconnection and dynamo

The RFP experiences robust reconnection through the occurrence of multiple tearing instabilities corresponding to multiple mode-resonant surfaces present in the plasma. The tearing instabilities also produce a dynamo effect: the generation of a mean (flux-surface-averaged) current within the plasma, parallel to the mean magnetic field. The profile of the current density within the plasma differs greatly from that expected from the electric field. The single-fluid MHD picture of reconnection and dynamo has been the dominant description of the RFP (see, e.g., [1]). In the past decade two-fluid effects on reconnection, particularly in simple geometry, have been studied theoretically (see, e.g., [2]). Recently, a quasilinear calculation has demonstrated that the Hall effect can significantly affect the tearing mode dynamo [3]. The Hall effect on the dynamo can be illustrated through the parallel, mean-field Ohm's law,

$$\langle E \rangle_{\parallel} + \langle \delta v \times \delta B \rangle_{\parallel} - \frac{\langle \delta j \times \delta B \rangle_{\parallel}}{ne} = \eta \langle j \rangle_{\parallel}, \quad (1)$$

where  $\langle \rangle$  denotes a flux-surface-average,  $\parallel$  denotes the component parallel to the mean magnetic field and  $\delta$  denotes a fluctuating quantity. In standard plasmas, the electric field term on the LHS is observed to be insufficient to balance the plasma current on the RHS (as discussed in section 3.1). The remaining terms on the LHS represent fluctuation-induced dynamo effects. The second term on the LHS is the MHD dynamo, while the third term is called the Hall dynamo.

Prior measurements of the MHD dynamo have indicated that it can account for the observed current in the edge plasma (as measured with various insertable probes at  $r/a > 0.9$ ,

where  $a$  is the plasma radius [4,5]) and is important in the core (as measured by chord-averaged spectroscopy [6]). However, the edge measurements also indicate that the MHD dynamo might become small at  $r/a \approx 0.85$ . The core spectroscopic measurements do not yet reveal the spatial structure of the MHD dynamo. Hence, these earlier measurements imply that an additional dynamo mechanism is also active. Quasilinear calculation of the Hall dynamo term shows that it can be much larger than the MHD dynamo, but more localized to a resonant surface [3].

We have measured the Hall dynamo in the plasma core using an eleven-chord laser Faraday rotation diagnostic [7]. The rotation of the laser beam electric field vector is proportional to the path integral  $\int (nB) dl$ , where  $n$  is the electron density and  $B$  is the magnetic field parallel to the beam path. The contribution of density fluctuations to the integral for the six laser chords nearest the plasma core is small, due to the small magnitude of the fluctuations, their  $m = 1$  structure, and the small magnitude of the mean magnetic field parallel to the beam path. Hence, from proper inversion of the path integrals (for  $m = 1$  fluctuations), we can infer the  $m = 1$  magnetic and current density fluctuations [8]. To distill the dominant toroidal mode from the total signal, we correlate the Faraday rotation signal with the  $n = 6$  mode measured by the toroidal array of magnetic pick-up coils at the plasma boundary. The  $m = 1$ ,  $n = 6$  magnetic fluctuations (figure 1) are found to be radially global, with the poloidal component reversing direction at the mode resonant ( $q = \frac{1}{6}$ ) surface, as expected for a classical tearing mode. The  $m = 1$ ,  $n = 6$  current density fluctuation is much more localized, also as expected for a tearing mode. However, the width is approximately  $8 \pm 3$  cm, larger than the linear MHD expectation.

In MST, the magnetic fluctuations and mean quantities undergo a sawtooth cycle. For example, it is seen in figure 2(a) that the current density fluctuations peak during a sawtooth crash. The dynamo strength varies through the cycle, also peaking in the vicinity of the crash phase. The Hall dynamo is measured by correlating the current and magnetic field fluctuations over an ensemble of 300 sawtooth cycles. Since the tearing modes are rotating, the ensemble average approximates a magnetic surface average. The Hall dynamo is measured to become large (up to  $40 \text{ V m}^{-1}$ ) during the sawtooth crash (figure 2(b)). Simultaneously, the toroidal magnetic flux is amplified, reflecting the dynamo action (figure 2(d)). The mean electric field (figure 2(c)) also becomes large during a sawtooth crash, comparable to the Hall dynamo, a result of the redistribution of the magnetic field. However, the Hall dynamo in the core is directed opposite to the electric field. The sum of the Hall dynamo and the electric field is of the appropriate magnitude to account for the measured current (the current density term in equation (1) is small compared to the other terms in the equation). Thus, the Hall effect in MST contributes significantly to reconnection and dynamo in MST. The precise, relative roles of MHD and Hall effects await further measurements with improved spatial resolution.

### 2.2. The origin of the $m = 0$ edge-resonant mode

The dominant unstable modes in the RFP are the global, core-resonant,  $m = 1$  tearing modes. Typically, there are several

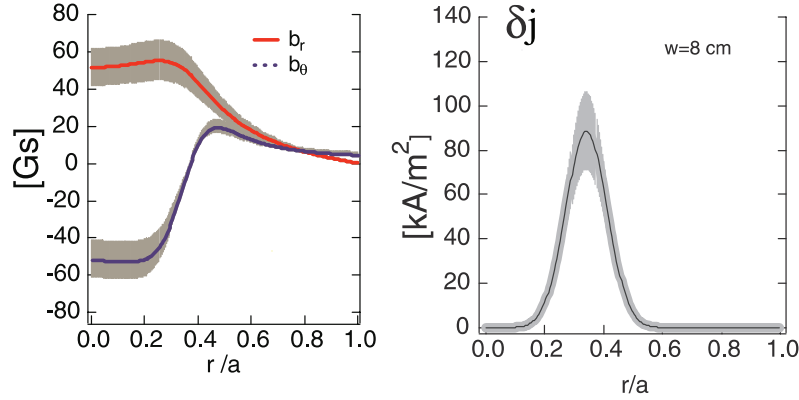


**Figure 1.** Radial profiles of radial and poloidal magnetic fluctuations (left figure) and toroidal current density fluctuations (right figure). The fluctuations are obtained from inversion of laser Faraday rotation data. The current measurement assumes a Gaussian profile for the inversion.

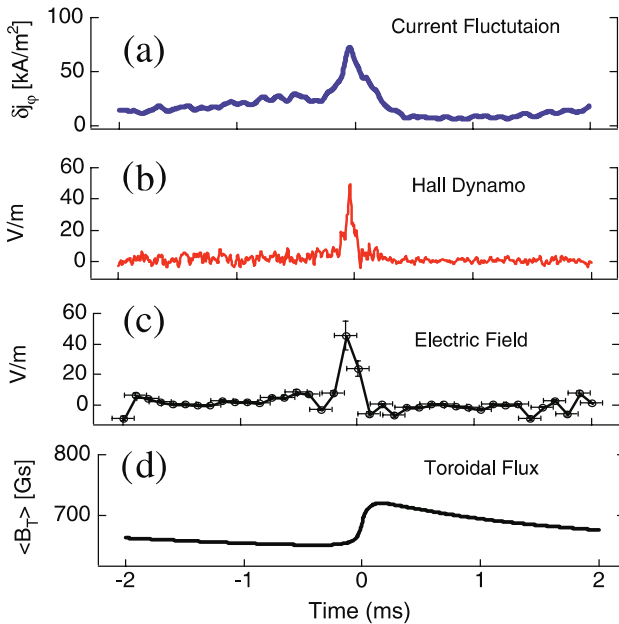


**Figure 2.** (a) Toroidal current density fluctuations, (b) Hall dynamo  $\langle \delta j \times \delta B \rangle_{\parallel} / ne$ , (c) parallel mean electric field and (d) toroidal magnetic flux versus time through a sawtooth cycle. As seen from equation (1), the effects of the Hall and electric field forces are opposing.

nonlinearly coupled modes that dominate. In MST the  $m = 1$ ,  $n = 6-8$  modes are large. Their amplitudes grow prior to a sawtooth crash (figure 3(b)). During a sawtooth crash, the  $m = 0$  mode (with  $n$  dominantly unity) occurs as a strong burst in time, as shown in figure 3(c). The  $m = 0$  mode is resonant at the  $q = 0$  surface, which is near the plasma edge at  $r/a \approx 0.85$ . The  $m = 0$  mode is important to RFP dynamics since it is responsible for the edge dynamo current; it mediates nonlinear coupling between different  $m = 1$  modes, and it may influence edge energy transport. It has been predicted by nonlinear MHD computation to be linearly stable, but generated by nonlinear coupling from two  $m = 1$  modes.

To determine the cause of the mode experimentally, we have measured the linear MHD drive term of the  $m = 0$  mode directly, through probe measurements in the edge plasma. The MHD equation for the evolution of the  $m = 0$ ,  $n = 1$

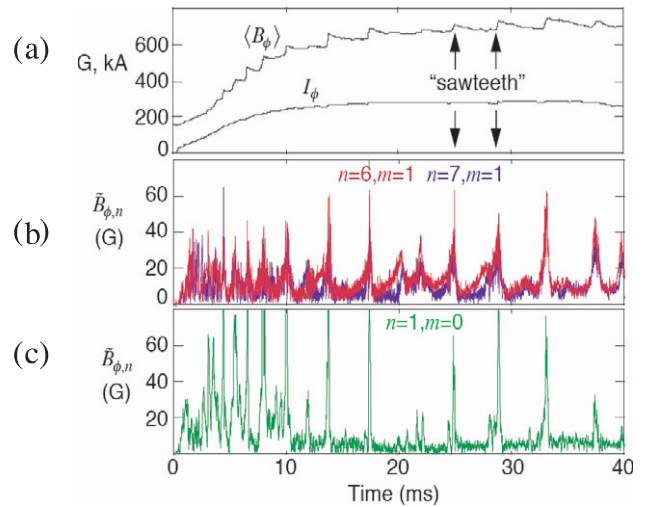


**Figure 3.** Time dependence of (a) toroidal flux and plasma current, (b) core-resonant magnetic  $m = 1$  magnetic fluctuations and (c) edge-resonant  $m = 0$  magnetic fluctuations.

modal energy can be written as

$$\frac{\partial \langle B_{0,1}^2 \rangle}{\partial t} = \langle \vec{B}_{0,1} \cdot \nabla \times (v_{0,1} \times \langle B \rangle) \rangle + \text{nonlinear terms} + \text{dissipation}, \quad (2)$$

where only the linear term is shown explicitly. We have measured the linear term (the first term on the RHS) for  $r/a > 0.9$  (using cylindrical coordinates to evaluate the derivative operator). The magnetic field is measured with magnetic probes and the flow velocity is measured with Langmuir probes, assuming that the fluctuating flow is a fluctuating  $E \times B$  drift. In both the experiment and resistive MHD computation, the flow is dominated by the  $E \times B$  drift from electrostatic fields. We see in figure 4(b) that the linear term is negative. Hence, we observe, in agreement with resistive MHD theory, that the  $m = 0$  is linearly damped. Its growth arises either from nonlinear mode coupling or a non-MHD instability. Measurement of the nonlinear term is underway.

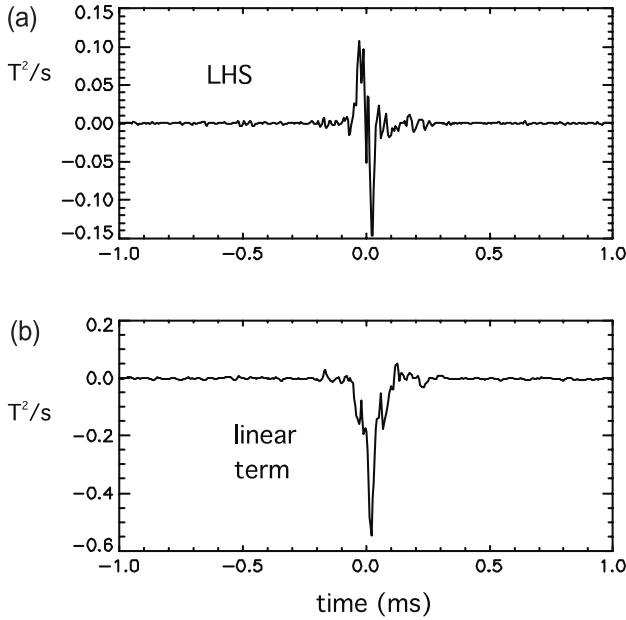


**Figure 4.** (a) Left-hand side of equation (2) and (b) linear drive term for the  $m = 0$  mode on the right-hand side versus time through a sawtooth crash.

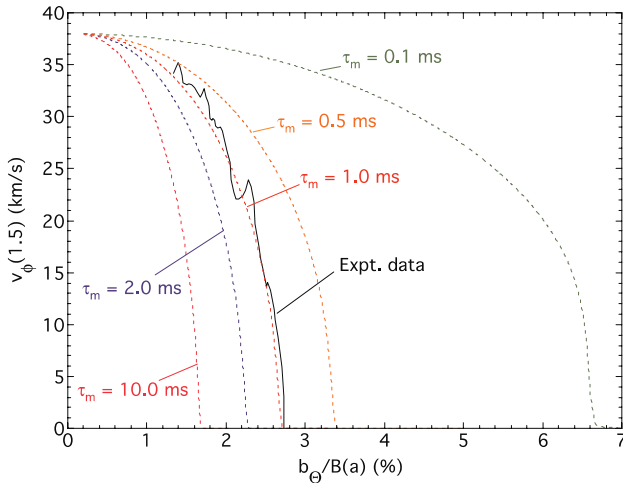


**Figure 5.** Trajectory of toroidal velocity versus poloidal magnetic fluctuation amplitude for the  $m = 1, n = 5$  mode (—), as the mode rotation decreases, and theoretical predictions for trajectory, based on torques from shell eddy current, for different values of the momentum confinement time,  $\tau_m$ .

### 2.3. Locking of tearing modes by wall eddy current

The slowing and locking of modes in the laboratory frame is a common occurrence in tokamaks and RFPs. In MST, discharges can be produced with time periods in which one tearing mode is dominant. In such discharges, the rotation of the dominant mode decreases over several milliseconds, and the mode eventually locks. A time trajectory of the  $m = 1, n = 5$  mode velocity versus the mode amplitude is shown in figure 5. It is seen that as the mode amplitude increases the mode decelerates. It has been determined that the mode braking is due to the torque from eddy current in the surrounding metal shell. The braking is not due to the error magnetic field.

The helical current associated with the tearing mode can induce an image current in a surrounding conducting shell. If the shell resistivity is finite, the image current develops a phase difference from the helical current within the plasma. The image (or eddy) current induces a resonant current response at the mode-resonant surface. The resulting local Lorentz force can decelerate the plasma in the vicinity of the resonant surface. The deceleration is opposed and distributed radially by viscous forces within the plasma. Hence, the deceleration of the plasma (and the mode that rotates at a fixed speed in the plasma frame) is determined by the eddy current braking force and the viscous force. The theory was developed for the tokamak [8, 9], and also applied to the RFP [10]. We have tested the eddy current braking theory against MST results [11]. The theory has essentially one free parameter: the plasma viscosity parametrized as a global momentum confinement time,  $\tau_m$ . The prediction of the theory for various momentum diffusivities is shown in figure 5. The momentum confinement time has been inferred experimentally by inducing flow with a biased electrode and observing the viscous decay, yielding  $\tau_m \sim 1.5$  ms [12]. From figure 5 we see that invoking the measured confinement time yields an excellent match between theory and experiment for the time history of the mode rotation.

### 3. Reduction of relaxation with improved confinement

In recent years, confinement has improved greatly in the RFP through current density profile control (see, e.g., [13]). In the standard RFP the parallel electric field is strongly peaked at the centre. The peaking arises from the projection of the applied toroidal electric field along the strongly sheared magnetic field. The resulting peaked current density profile is unstable to tearing instabilities. The instabilities grow and force the current density profile to one that is less peaked. The magnetic fluctuations in the saturated state cause substantial transport.

To improve confinement, the applied electric field is adjusted so that the plasma current induced by the electric field is less peaked, yielding a more stable plasma with smaller fluctuations. During a plasma discharge an additional Ohmic electric field is applied that has a strong parallel (mostly poloidal) component in the outer region of the plasma, a technique that is often referred to as pulsed parallel current drive (PPCD). The results are dramatic: the energy confinement time increases from 1 ms to roughly 10 ms, beta (the ratio of volume averaged pressure to surface magnetic pressure) increases from 9% to 15%, core electron temperature increases about threefold (reaching 1.3 keV at high current), energetic electrons become well-confined up to the measured energies of 100 keV and electron diffusivity (inferred from Fokker-Planck modelling of hard x-ray emission) indicates a velocity-independent diffusivity (inconsistent with expectations for transport from stochastic fields). The value of the energy confinement time is comparable to that of a tokamak of similar size and plasma current [14, 15]. In the following three sections we report new results of plasma behaviour in this improved confinement regime.

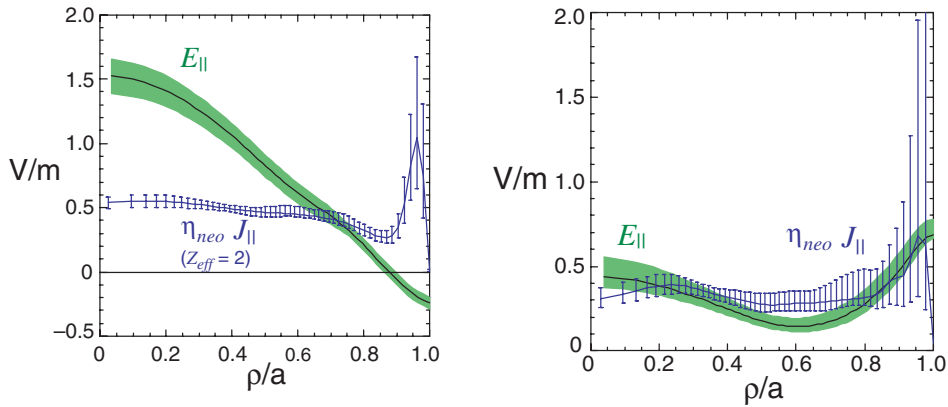


**Figure 6.** Radial profile of mean electric field and current density terms in Ohm's law for (a) standard plasmas and (b) PPCD plasmas. The difference between the two curves indicates the dynamo effect.

### 3.1. Suppression of the dynamo

The large magnetic fluctuations that accompany standard RFP plasmas produce a strong dynamo effect, as discussed in section 2.1. With improved confinement, the dynamo is strongly reduced. The presence of the dynamo is most clearly seen through measurement of the terms in the parallel mean-field Ohm's law obtained during the sawtooth-free improved confinement period. Figure 6 shows the measured radial profiles of the parallel electric field and current density terms in Ohm's law. The quantities are evaluated from an equilibrium reconstruction code with a large set of diagnostic inputs to constrain the solution, including Faraday rotation and motional Stark effect diagnosis for magnetic field information and Thomson scattering and laser interferometry for plasma pressure. The electric field is evaluated by a new reconstruction technique employing the time derivative of the Grad-Shafranov equation [16]. Neoclassical resistivity is employed, with the profile of the effective ionic charge ( $Z_{\text{eff}}$ ) determined in PPCD plasmas from near-infrared bremsstrahlung radiation. In standard plasmas, the radiation spectrum is contaminated by emission from neutrals. Hence, we assume a constant  $Z_{\text{eff}}$  profile, but choose its value to match the overall measured Ohmic input power. The value of  $Z_{\text{eff}}$  in the standard plasma is then 2, reduced from the central value in PPCD plasmas of 4.7. The uncertainty in  $Z_{\text{eff}}$  does not affect the overall conclusions.

In standard plasmas (figure 6(a)) the current density profile is very different from the electric field profile. In the core, the current density is smaller than would be expected from the electric field, while at the edge the current density is directed opposite to the electric field. A strong dynamo exists, which drives current opposite to the electric field over much of the cross-section. The data presented are obtained between sawtooth crashes. In PPCD plasmas (figure 6(b)) the electric field profile changes substantially and, within experimental uncertainty, the current is fully accounted for by the applied electric field over most of the plasma cross section. Hence, we have produced an RFP plasma that is essentially dynamo-free [16]. The Hall dynamo, discussed earlier, is also reduced in these plasmas. In addition, the electrical resistivity is approximately given by the neoclassical prediction.

The PPCD measurements are also consistent with the interpretation of the cause of the reduced fluctuations and

improved confinement. In standard plasmas, the electric field in figure 6(a) is peaked, forming a current density profile that is unstable to tearing instability. The resulting fluctuations, through the dynamo electromotive force, then limit the peaking of the current profile, so that the current density profile becomes broader than would be expected from the electric field alone. The resulting current density profile, composed of electric-field-driven current and dynamo-driven current, is close to marginal stability. In PPCD plasmas the applied electric field is measured to be much flatter (figure 6(b)), as intended. This drives a flatter current density profile for improved stability. However, the current density profile is only slightly different from the standard case since the current density profile produced by the electric field is already near marginal stability. The larger change occurs in the electric field profile. The electric field experiences a large inductive change that accompanies the time-varying equilibrium arising from the programming of the poloidal and toroidal surface loop voltages. The improved stability of the electric-field-driven current profile yields reduction in tearing instability and improvement in confinement.

### 3.2. Appearance of isolated magnetic islands

The standard RFP plasma consists of multiple tearing modes resonant at multiple magnetic surfaces. The calculated magnetic islands are sufficiently broad that the islands overlap and produce a stochastic magnetic field. Nonlinear MHD computation predicts a stochastic magnetic field. However, the magnetic fluctuations are sufficiently small that a field line travels many times around the torus prior to reaching the plasma edge. Thus, energy loss is constrained (the energy confinement time in standard MST plasmas is about 1 ms).

The magnetic structure can be inferred from soft x-ray emission, measured with a pinhole camera with twelve lines of sight [17]. In standard plasmas, contours of constant soft x-ray emission are nested tori (figure 7(a)). Magnetic islands are not observed since the magnetic field is stochastic. In PPCD plasmas, the fluctuations are reduced and the magnetic field becomes substantially less stochastic. Soft x-ray emissivity reveals the presence of islands (figure 7(b)). We observe two magnetic islands, corresponding to the locations of the  $m/n = 1/6$  and  $1/7$  mode resonant surfaces. The island presence

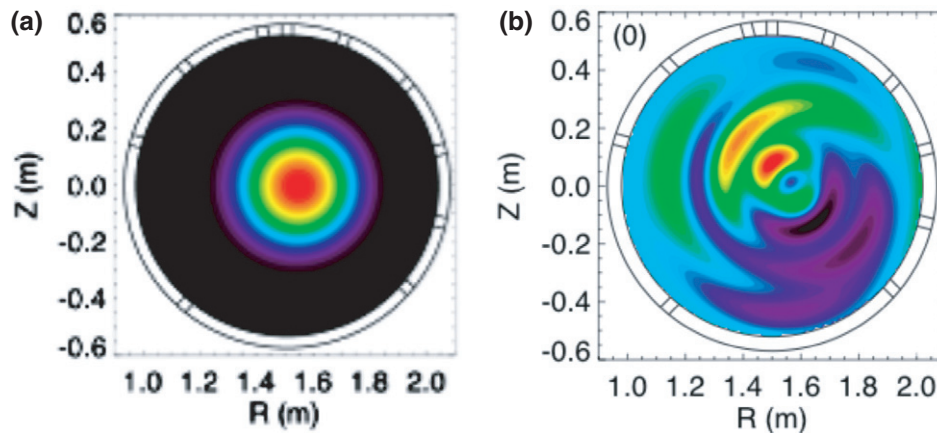


**Figure 7.** Contours of constant soft x-ray emissivity, in the poloidal plane, for (a) standard and (b) PPCD plasmas. For (b) the mean signal is subtracted, so that the fluctuating islands are visible (red islands indicate a positive value and blue a negative value, relative to the mean).

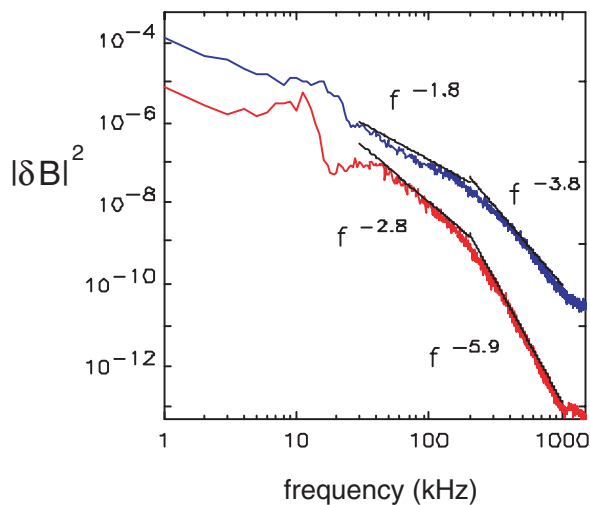


**Figure 8.** Frequency spectrum of magnetic fluctuations for standard plasmas (top curve) and PPCD plasmas (bottom curve). The straight lines, described by the power laws shown, are fits to the data.

in soft x-ray emissivity is consistent with the magnetic puncture plot (not shown) obtained from the measured surface magnetic fluctuations, with radial profiles obtained from tearing mode eigenfunctions. Thus, it is clear that improved confinement PPCD plasmas contain reduced stochasticity.

### 3.3. Reduction of high frequency magnetic turbulence

At frequencies higher than those of the tearing instabilities ( $f > 30$  kHz) the magnetic fluctuation spectrum is broadband and turbulent. The origin of the turbulence is unknown. However, we report here two interesting features of the turbulence, and its changes with improved confinement. First, the turbulence amplitude decreases from standard to PPCD plasmas, as shown in figure 8. The goal of current profile control is to reduce the large core-resonant tearing modes that contribute significant transport and occur in the vicinity of 10 kHz. However, we also observe a significant reduction in the higher frequency turbulence. This suggests that there may be a link between the turbulence and the tearing

modes, perhaps consistent with generation of the turbulence from nonlinear coupling from the large-scale modes. Second, in standard plasmas the magnetic turbulence is not self-similar and displays intermittency [18], as previously observed for edge electrostatic fluctuations and particle transport in the RFP [19, 20]. This is revealed by measuring the probability distribution function (PDF) of the difference signal,  $\delta B(t) - \delta B(t + \tau)$ , which is observed to vary with the time delay,  $\tau$ . In contrast, in PPCD the fluctuations become self-similar (PDF independent of  $\tau$ ) and intermittency is reduced.

## 4. Progress with new auxiliary control techniques

Several new techniques are advancing in MST to improve control of the current density profile, heat the plasma and sustain the plasma current. For current profile control and heating we are developing two RF wave techniques for the RFP (lower hybrid and electron Bernstein wave injection) and neutral beam injection. For lower hybrid current drive an antenna has been developed that meets the stringent requirements of MST (small radial antenna extent and small portholes). An interdigital, slow wave antenna is installed and operating at 75 kW. For electron Bernstein wave injection a twin waveguide antenna operates successfully. Coupling measurements agree with theory at very low power (10 W) and experiments are now underway at 100 kW. For both RF techniques power will be increased to several hundred kilowatts over the next year for tests of the feasibility of current drive in the RFP. The feasibility of neutral beam injection is being tested with a 1 MW, 1 ms beam. The key issue is the relative values of the fast ion confinement time and slowing down time. For sustainment of the bulk current we are applying ac helicity injection (also known as OFCD). In OFCD, the surface poloidal and toroidal loop voltages are oscillated  $90^\circ$  out of phase. This injects and sustains the magnetic helicity in the plasma. Three-dimensional MHD simulation of OFCD indicates that the technique can sustain the plasma current, although the influence on magnetic fluctuations may be a concern. To date, experimental results at moderate power demonstrate sustainment of a small amount of the total current (figure 9), consistent with theoretical expectations.

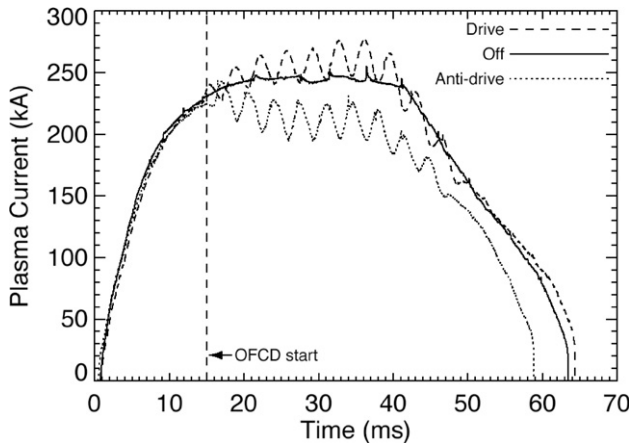


**Figure 9.** Plasma current versus time for three cases: OFCD with toroidal and poloidal loop voltages relative phases set for maximum helicity injection (---), OFCD with voltage phase set for maximum helicity removal and OFCD off.

Finally, we are injecting frozen deuterium pellets for central fuelling. To date, pellets are able to increase density in PPCD plasmas beyond previous values, while maintaining magnetic fluctuations at their reduced level.

## 5. Concluding remarks

The RFP is able to operate in two different physics regimes. The standard regime offers substantial opportunity to investigate physics of magnetic self-organization. We have reported here results on Hall effects on dynamo and reconnection, the origin of the  $m = 0$  edge-resonant mode, and mode braking by eddy currents in the shell. In improved confinement PPCD plasmas, all activity driven by magnetic fluctuations is highly suppressed. We have reported changes in dynamo activity, magnetic surface structure inferred from soft x-ray tomography and high frequency magnetic turbulence. Determination of the underlying physics of the improved confinement regime is only just beginning, and may be dominated by electrostatic fluctuations.

The large change in RFP confinement and magnetic relaxation was enabled by a coarse form of transient current

profile control (programming of the Ohmic loop voltages). RFP research will benefit strongly from the application of auxiliary current drive and heating. Thus, a program is underway on MST to apply RF techniques (lower hybrid and electron Bernstein waves), neutral beam injection and OFCD. Each of these techniques is underway at low or moderate power, with advances to high power dependent on unfolding results. These will be used to determine the ultimate limits to confinement and beta in the RFP, and further to control RFP behaviour.

## References

- [1] Ortolani S. and Schnack D. 1993 *Magnetohydrodynamics of Plasma Relaxation* (Singapore: World Scientific)
- [2] Biskamp D. 2000 *Magnetic Reconnection in Plasmas* (Cambridge: Cambridge University Press)
- [3] Mirnov V., Hegna C. and Prager S. 2003 *Plasma Phys. Rep. (Fiz. Plazmy)* **29** 566
- [4] Ji H., Almagri A.F., Prager S.C. and Sarff J.S. 1994 *Phys. Rev. Lett.* **73** 668
- [5] Fontana P. W., Den Hartog D.J., Fiksel G. and Prager S.C. 2000 *Phys. Rev. Lett.* **85** 566
- [6] Den Hartog D.J., Chapman J., Craig D., Fiksel G., Fontana P.W., Prager S.C. and Sarff J.S. 1999 *Phys. Plasmas* **6** 1813
- [7] Ding W.X., Brower D.H., Craig D., Deng B., Fiksel G., Mirnov V., Prager S.C., Sarff J.S. and Svidzinski V. 2004 *Phys. Rev. Lett.* **93** 045002
- [8] Nave M.F.F. and Wesson J.A. 1990 *Nucl. Fusion* **30** 2575
- [9] Fitzpatrick R. 1993 *Nucl. Fusion* **33** 1049
- [10] Fitzpatrick R., Guo S.C., Den Hartog D.J. and Hegna C.C. 1999 *Phys. Plasmas* **6** 3878
- [11] Chapman B.E., Fitzpatrick R., Craig D., Martin P. and Spizzo G. 2004 *Phys. Plasmas* **11** 2156
- [12] Almagri A.F., Chapman J.T., Chang C.S., Craig D., Den Hartog D.J., Hegna C.C. and Prager S.C. 1998 *Phys. Plasmas* **5** 3982
- [13] Chapman B.E. *et al* 2002 *Phys. Plasmas*. **9** 2001 and references therein
- [14] Sarff J. *et al* 2003 *Nucl. Fusion* **43** 1684
- [15] Sarff J. *et al* 2003 *Plasma Phys. Control. Fusion* **45** A457
- [16] Anderson J.K., Biewer T.M., Forest C.B., O'Connell R., Prager S.C. and Sarff J.S. 2004 *Phys. Plasmas* **11** 19
- [17] Franz P. *et al* 2004 *Phys. Rev. Lett.* **92** 125001
- [18] Marrelli L., Frassinetti L., Martin P., Craig D. and Sarff J.S. 2005 *Phys. Plasmas* **12** 030701
- [19] Spada E. *et al* 2001 *Phys. Rev. Lett.* **86** 3032
- [20] Antoni V. *et al* 2001 *Phys. Rev. Lett.* **87** 045001